Journal of Applied Physics

Electromagnetic enhancement effect on the atomically abrupt heterojunction of Si/InAs heterostructured nanowires

Cite as: J. Appl. Phys. **125**, 064303 (2019); https://doi.org/10.1063/1.5058276
Submitted: 18 September 2018 . Accepted: 20 December 2018 . Published Online: 13 February 2019

J. L. Pura, A. J. Magdaleno, D. Muñoz-Segovia, M. Glaser, A. Lugstein, and J. Jiménez

AIP Publishing

Journal of Applied Physics ARTICLE scitation.org/journal/jap

Electromagnetic enhancement effect on the atomically abrupt heterojunction of Si/InAs heterostructured nanowires

Cite as: J. Appl. Phys. **125**, 064303 (2019); doi: 10.1063/1.5058276
Submitted: 18 September 2018 · Accepted: 20 December 2018 ·
Published Online: 13 February 2019

J. L. Pura,[1,a)] A. J. Magdaleno,[1] D. Muñoz-Segovia,[1] M. Glaser,[2] A. Lugstein,[2] and J. Jiménez[1]

AFFILIATIONS

[1]GdS Optronlab, Dpt. Física de la Materia Condensada, ed. LUCIA Universidad de Valladolid, Paseo de Belén 19, 47011 Valladolid, Spain
[2]Institute for Solid State Electronics, Vienna University of Technology, Floragasse 7, 1040 Vienna, Austria

Note: This paper is part of the Special Topic on: Dielectric Nanoresonators and Metamaterials.
[a)]**Email:** jlpura@fmc.uva.es

ABSTRACT

Semiconductor nanowires (NWs) present a great number of unique optical properties associated with their reduced dimension and internal structure. NWs are suitable for the fabrication of defect free Si/III-V heterostructures, allowing the combination of the properties of both Si and III-V compounds. We present here a study of the electromagnetic (EM) resonances on the atomically abrupt heterojunction (HJ) of Si/InAs axially heterostructured NWs. We studied the electromagnetic response of Si/InAs heterojunctions sensed by means of micro-Raman spectroscopy. These measurements reveal a high enhancement of the Si Raman signal when the incident laser beam is focused right on the Si/InAs interface. The experimental Raman observations are compared to simulations of finite element methods for the interaction of the focused laser beam with the heterostructured NW. The simulations explain why the enhancement is detected on the Si signal when illuminating the HJ and also provide a physical framework to understand the interaction between the incident EM field and the heterostructured NW. The understanding of this process opens the possibility of controlling the light absorption/scattering on semiconductor NWs with the use of heterostructures while taking advantage of the properties of both Si and III-V semiconductors. This is important not only for current NW based photonic nanodevices, such as light sensors, but also for the design of new optoelectronic devices based on NWs.

INTRODUCTION

Semiconductor nanowires (NWs) exhibit unique physical properties as a consequence of their confined dimension, the diameter. Besides, the presence of heterojunctions (HJ) is necessary for building up electronic and optoelectronic nanodevices.[1–4] Among all the possible heterostructured NWs, those based on Si are especially interesting because of its useful properties for solar applications, versatility, and the possibility of their integration with the already existing Complementary Metal Oxide Semiconductor (CMOS) technology. According to this, a great variety of Si NW based devices has been produced, e.g., Si NW near-infrared photodetectors[5] or double-gated Si NW FET sensors.[6] On the other hand, III-V semiconductors present higher values of the carrier mobility and improved optical properties with respect to their group IV counterparts, thus making up for Si drawbacks. The integration of Si/III-V heterostructures in a single NW would allow combining the advantages of both Si and III-V semiconductors with the unique optical properties of semiconductor NWs.[7–11]

III-V semiconductor NWs are being extensively investigated for its possible applications on nanowire solar cells[12,13] and light sources, including lasers.[14–18] There are excellent studies of InP NWs, based on their optical properties and resonances,[19] and its high efficiency as solar cells.[20] Also, as an example of Si/III-V integration, InAs NWs deposited on a Si substrate were used in photovoltaics and photodetectors.[21]

In previous works, we reported the enhancement of the Raman signal at the heterojunction of axially heterostructured Si/SiGe nanowires.[22] We demonstrated that the enhancement effect appears as a result of the interaction between the incident electromagnetic (EM) field and the dielectric discontinuity at the heterojunction.[23,24] According to this, the EM enhancement effect is expected to appear in any kind of axially heterostructured NW. In this work, we will study the electromagnetic behavior of heterostructured Si/InAs NWs using micro-Raman spectroscopy as a probe of the EM field inside the NW. A theoretical framework of the problem is established by solving the Maxwell equations of the light/NW system by Finite Element Methods (FEM). Finally, the results of the simulations are contrasted with the micro-Raman experiments.

EXPERIMENTAL AND SAMPLES

The Si/InAs heterostructured NWs were fabricated with an ion implantation and a flash annealing procedure, similar to the one presented in Ref. 4. The ⟨111⟩ oriented Si NWs were epitaxially grown on Si (111) substrates by applying the gold-catalyzed vapour-liquid-solid (VLS) method. After removal of gold by wet chemical etching, approximately 20 nm SiO_2 was deposited on the NWs by plasma enhanced chemical vapour deposition, acting as a protecting layer for the following steps. In order to achieve homogeneous implantation profiles along the NWs, samples were placed on a 45° tilted and continuously rotating stage during the ion implantation. In and As ions were implanted alternatingly with an energy of 120 keV and 90 keV, respectively. The recrystallization along with the phase separation and formation of Si/InAs heterostructures within the NW core was finally achieved by applying a 20 ms flash lamp annealing step with a flash energy of about 50 J/cm^2.

The NW morphology and structure were studied in a high-resolution Field Emission Scanning Electron Microscope (FESEM). Heterostructured NWs appear as straight cylinders with slight tapering. The InAs segment is shorter than the Si segment, namely, 200–500 nm vs 3–4 μm. Energy-Dispersive X-ray Spectroscopy (EDS) was used to determine the NW composition, revealing that the brighter regions in the SEM micrographs are indeed InAs, while the darker contrast segment consists of Si, as expected from different atomic numbers (see Fig. 1).

Raman spectra profiles along the axes of several Si/InAs NWs were obtained in order to study the effect of the heterojunction on the Raman signal. The laser excitation was performed with a continuous wave frequency doubled Nd:YAG laser (532 nm) going through a 100× objective; this gives a laser spot of ~1 μm. The maximum laser power was 450 μW (~14 kW/cm^2), and non-linear effects are not detected at this power level (although they might appear for higher power). During the Raman measurements, the NWs are lying over an Al coated Si substrate, so the excitation beam is always perpendicular to the NW axis and the substrate. The laser polarization is always parallel to the NW axis in order to record the maximum Raman signal. The Raman spectra were recorded along the NW axis in steps of 200 nm. Further details about the experimental method followed for the characterization of the heterostructured NWs can be found elsewhere.[22,23] The typical Raman spectrum of these NWs when the HJ is being excited by the laser beam will contain the Raman bands of both crystalline Si and InAs (Fig. 2). When each individual segment of the NW is illuminated, only the signal of the semiconductor forming the segment is recorded. The spectrum of the Si NW segment consists of the degenerated LO and TO modes located at 520.6 cm^{-1},

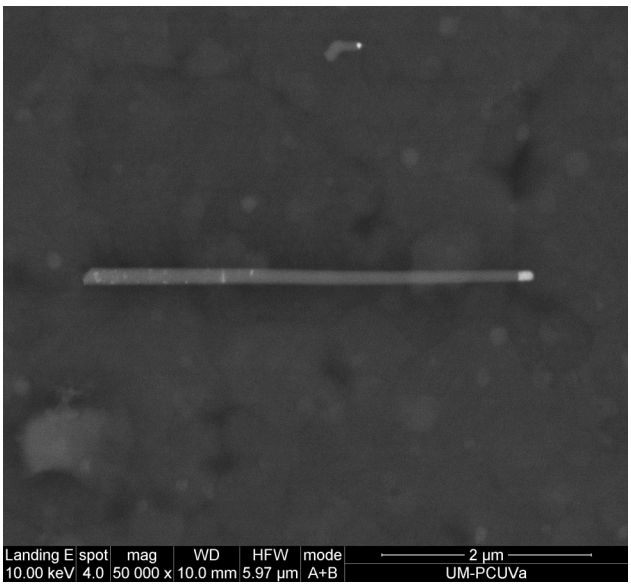

FIG. 1. SEM image of a typical Si/InAs heterostructured NW. The InAs segment can be detected on the right side as a brighter region on the NW.

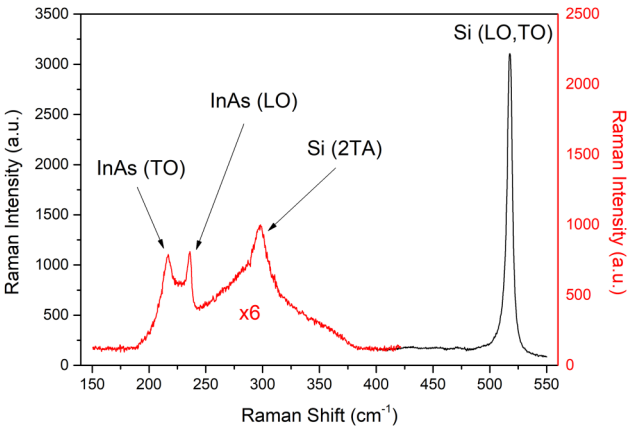

FIG. 2. Typical Raman spectrum of a Si/InAs NW when the HJ region is illuminated. It shows the principal Raman bands of both NW segments, Si and InAs.

labeled Si (LO,TO), and the much less intense second order transverse acoustic mode around 300 cm^{-1}, labeled Si (2TA). For the InAs segment, we can observe the LO and TO modes at 217.3 cm^{-1} and 238.6 cm^{-1}, respectively.[25]

RESULTS

We acquired the Raman profiles along the axis of several Si/InAs NWs. Then, the intensities of the different Raman bands were extracted from each spectrum. This allows visualizing the dependence of the Raman signals as a function of the laser beam position along the NW. Two examples of the Raman intensity profiles are shown in Fig. 3, corresponding to two different Si/InAs heterostructured NWs.

Both profiles show that the Raman intensities arising from the Si segment are enhanced when the HJ region is illuminated by the laser beam, giving enhancement factors of 25 and 10 times, respectively. This enhancement factor is calculated as the ratio between the maximum Raman intensity recorded next to the HJ, with respect to the one recorded on the homogeneous Si segment of the NW. This proves that the enhancement effect is also present in Si/InAs heterostructured NWs, in spite of some differences with respect to the same effect observed in Si/SiGe NWs previously studied.[11,12] In the case of SiGe/Si heterostructured NWs, Si and Ge are both non-polar semiconductors, and the SiGe alloy is stable for any Si/Ge ratio. The full miscibility of Ge and Si and its high solubility in the catalyst metal are responsible for the graded HJs extending several tens of nanometres depending on the NW diameter.[26] The SiGe/Si heterojunction is not abrupt, but a continuous transition between the compositions of the two NW segments constitutes the heterojunction. Therefore, one can associate a certain volume of the material to the HJ region itself, which is chemically recognizable, and the Raman signal arising from this volume forming the HJ permitted to study the true local field enhancement (intensity per unit scattering volume). This situation does not apply to Si/InAs NWs, because the immiscibility between polar InAs and non-polar Si makes the Si/InAs heterojunction atomically abrupt.[27] For this reason, one cannot extract a spectrally differentiated signal arising from the HJ itself; however, the EM enhancement effect is clearly observed around the HJ in the profiles of Fig. 3. The Raman intensity of Si is strongly enhanced in the region of the Si NW segment adjacent to the heterojunction. The true EM enhancement per unit scattering volume is difficult to estimate, because of the limited spatial resolution of the micro-Raman probe. However, the increase of the Raman intensity around the HJ can be unambiguously appreciated in Fig. 3. It is important to note that any effect of the electronic states or resonance with the bandgap energy has been ruled out. This is because Si and InAs bandgaps are in the IR and far-IR regions, respectively, and the band alignment between both of them is type II.[28] As a result, any possible interaction between carriers will need both a change in momentum and position, which will drastically reduce its efficiency.

The experimental results have been contrasted with the EM field calculated by FEM simulations. The Maxwell equations were solved for the substrate/NW system; the FEM calculation provides us with the distribution of the electric field intensity, $|E|^2$, inside the NW. A more detailed explanation of the developed FEM model can be found in previous papers.[22,23] There are two main differences in Si/InAs heterostructured NWs with respect to Si/SiGe heterostructured NWs. First, as we mentioned, the axial heterojunctions for both types of NWs are different, graded for SiGe/Si and abrupt for InAs/Si. Second, InAs presents much higher dielectric losses (imaginary part of the refractive index, k) than Si or the SiGe alloy for light in the visible range (Table I). The values of the optical constants of InAs can be found in Ref. 29. The dimensions of the heterostructured NW used in the simulations are 100 nm, diameter; 500 nm,

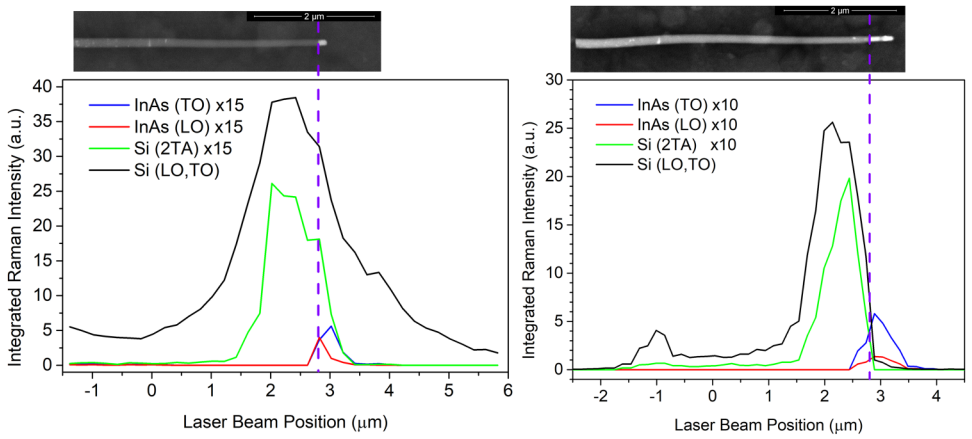

FIG. 3. Raman intensity profiles of two different Si/InAs heterostructured NWs. The upper SEM images have the same scale as the plots and show the position of the HJ. A strong enhancement of the Si signal arising from the Si region adjacent to the HJ can be seen.

TABLE I. Real (n) and imaginary (k) parts of the complex refractive indexes of the different materials used in the FEM calculations for 532 nm radiation.

	InAs	Si	$Si_{(1-x)}Ge_x$
n	4.3736	4.1334	$4.1334 + 0.668619x + 1.510779x^2$
k	1.0831	0.033258	$0.033258 - 0.204615x + 1.621028x^2$

the length of the InAs segment; and 3500 nm, the length of the Si segment.

The main results of the simulations are summarized in Fig. 4. The solution of the Maxwell equations provides the distribution of the EM field inside the NW. Figure 4(a) shows the volume distribution of the relative EM field intensity on the NW and its environment when the laser beam is focused on the HJ. The relative EM field is defined as the value of the EM field divided by the incident field, $|E|^2/|E_{inc}|^2$. Figure 4(b) shows the distribution of the same magnitude along the NW axis. We can see that the effect of the higher dielectric losses on the InAs side consists of a marked reduction of the EM field intensity with respect to the Si side next to the HJ. It explains the low InAs Raman signal detected on the experimental measurements, even next to the heterojunction. On the other hand, we can see the enhancement and localization of the incident field on the Si side. The EM field is enhanced by more than 3 times in a small region of about 300 nm, close to the heterojunction. One can establish here an estimation for the dimension of the NW region where the EM enhancement takes place; therefore, one can estimate the Raman intensity per unit volume to bring up the true EM enhancement at the HJ. Figure 4(c) presents the theoretical Raman intensity, which should be proportional to the excitation field intensity, i.e., $|E|^2$. This value is obtained from the simulation by varying the laser beam position along the NW axis and integrating on each of the NW segments. We can see that the intensity of the Si signal is enhanced when the laser beam approaches the HJ as compared to the calculated intensity obtained when illuminating the homogeneous Si segment. These results are in very good agreement with the experimental measurements of Fig. 3, both showing the enhancement of the Si Raman signal as a consequence of the illumination of the Si/InAs HJ by the focused laser beam.

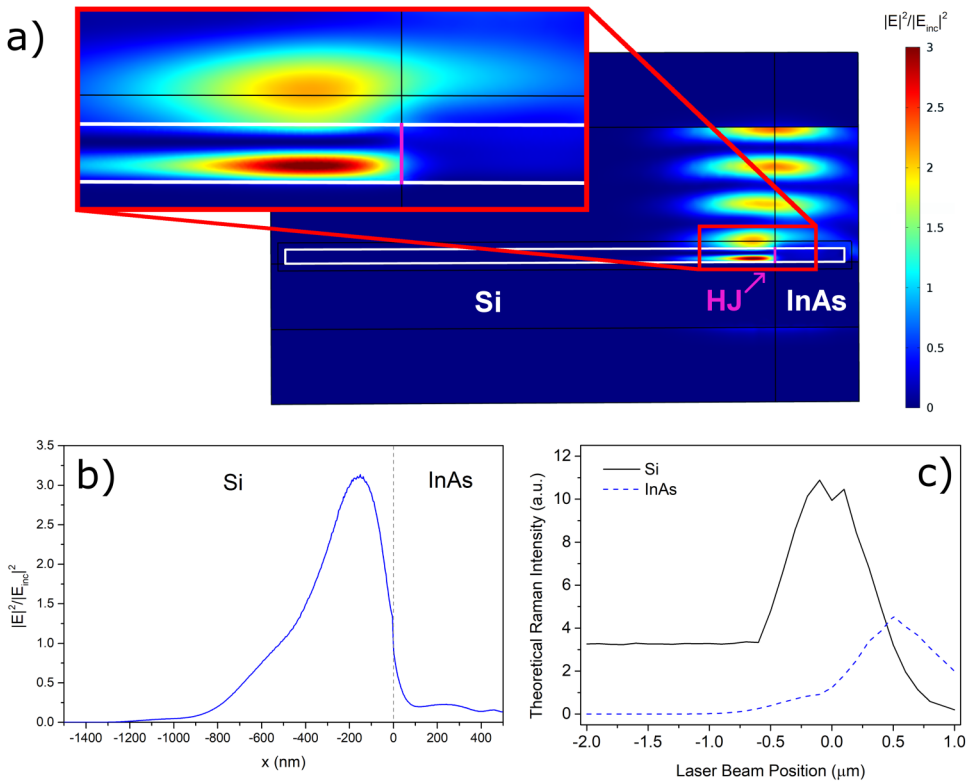

FIG. 4. (a) EM field distribution induced in a Si/InAs NW with a 100 nm diameter when the incident laser beam is focused on the HJ. The incident field is enhanced more than 3 times in a region of ~300 nm next to the HJ on the Si side. (b) Profile of the EM field distribution along the NW axis. (c) Simulation of the theoretical Raman signal as a function of the laser beam position to reproduce the experimental measurements of Fig. 3. Note that the high dielectric losses of InAs[29] ($k \sim 1$) result in a highly reduced field intensity in the InAs side.

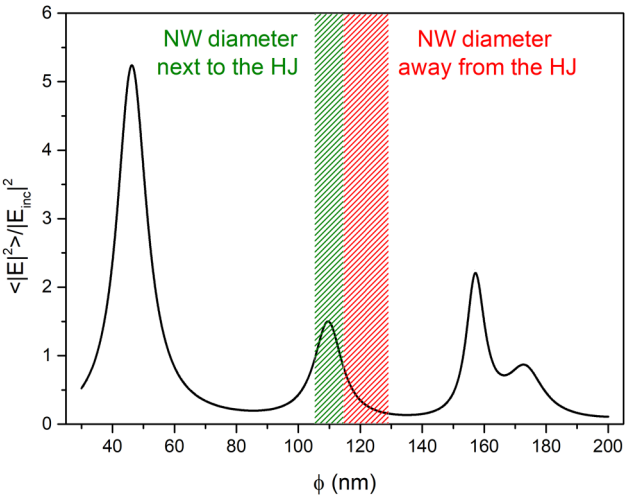

FIG. 5. Dependence of the mean value of the relative electric field intensity inside a pure Si NW as a function of its diameter. The studied Si/InAs NWs are tapered; as a result, the Si segment presents a smaller diameter in the region next to the HJ than in the region far away from the HJ. These two diameter ranges are represented by the shadowed regions, showing how a small diameter variation can shift out the diameter resonance of the Si segment in this case.

Finally, it is worth noting that the exact calculation of the experimental enhancement is difficult for two main reasons. First, the enhancement depends on the NW diameter. According to this, the response of a pure Si NW has been investigated. Figure 5 shows the average relative electric field inside a homogeneous Si NW as a function of its diameter. Si/InAs heterostructured NWs present a slight tapering (see Fig. 1); as a result, the diameter of the homogeneous Si segment becomes larger as it moves away from the HJ. Near the HJ, the NW diameter is around 100-120 nm, which coincides with a diameter resonance of Si (see Fig. 5). However, the NW diameter increases as we move away from the HJ, slightly deviating from the diameter resonance peak. This would explain the higher experimental values of the enhancement as compared to the homogeneous segment signal. The ratio between the two regions of Fig. 5 has a mean value of 5, which accounts for the observed difference between the experimental and theoretical values (a maximum value of 10 could be obtained when the diameter coincides exactly with the maximum of the resonance). On the other hand, the NW is not homogeneous, and it is covered by a SiO_2 outer shell, making the exact determination of the diameter even more difficult.

CONCLUSIONS

The Raman intensity is enhanced on the heterojunction of axially heterostructured Si/InAs NWs. The observation of this effect on different axially heterostructured NWs formed by different materials accounts for the description of this phenomenon as an EM effect associated with the dielectric discontinuity at the heterojunction. However, the detailed behavior of the EM enhancement effect strongly depends on the materials forming the HJ and the structure of the HJ itself. In the case of Si/SiGe NWs, the enhancement was detected on the signal arising from the HJ itself, which has a finite dimension. Alternatively, in Si/InAs NWs with abrupt HJs, the electromagnetic enhancement is observed in the region of the Si segment right next to the HJ. Note that the same effect also appears in the InAs side, but the high dielectric losses and reduced length of the InAs segment do not allow us to see the effect as clear as in the Si side. Both experimental and theoretical profiles of the EM field intensity along the NW show a higher intensity of the Si signal in the immediate vicinity of the HJ. The existence of this effect and its observation on very different materials suggest the possibility of detecting similar effects on other nanostructured systems with HJs. Finally, the enhanced absorption/scattering at the HJs in axially heterostructured NWs and its dependence with the NW composition and structure open interesting ways of photon handling using complex heterostructured NWs, with application in photon detection and photovoltaics, among others.

ACKNOWLEDGMENTS

This work was funded by Junta de Castilla y León (Project Nos. VA293U13 and VA081U16) and the Spanish Government [Nos. CICYT MAT2010-20441-C02 (01 and 02) and ENE 2014-56069-C4-4-R]. J. L. Pura was granted by the FPU program (Spanish Government) (No. FPU14/00916).

REFERENCES

[1]Y. Li, F. Qian, J. Xiang, and C. M. Lieber, "Nanowire electronic and optoelectronic devices," Mater. Today **9**(10), 18–27 (2006).
[2]Y. Cui, Z. Zhong, D. Wang, W. U. Wang, and C. M. Lieber, "High performance silicon nanowire field effect transistors," Nano Lett. **3**(2), 149–152 (2003).
[3]J. Xiang, W. Lu, Y. Hu, Y. Wu, H. Yan, and C. M. Lieber, "Ge/Si nanowire heterostructures as high-performance field-effect transistors," Nature **441**(7092), 489–493 (2006).
[4]M. Glaser, A. Kitzler, A. Johannes, S. Prucnal, H. Potts, S. Conesa-Boj, L. Filipovic, H. Kosina, W. Skorupa, E. Bertagnolli *et al.*, "Synthesis, morphological, and electro-optical characterizations of metal/semiconductor nanowire heterostructures," Nano Lett. **16**(6), 3507–3513 (2016).
[5]K. Das, S. Mukherjee, S. Manna, S. K. Ray, and A. K. Raychaudhuri, "Single Si nanowire (diameter≤100 Nm) based polarization sensitive near-infrared photodetector with ultra-high responsivity," Nanoscale **6**(19), 11232–11239 (2014).
[6]F. Gasparyan, H. Khondkaryan, A. Arakelyan, I. Zadorozhnyi, S. Pud, and S. Vitusevich, "Double-gated Si NW FET sensors: Low-frequency noise and photoelectric properties," J. Appl. Phys. **120**(6), 064902 (2016).
[7]K. Tomioka, M. Yoshimura, and T. Fukui, "A III-V nanowire channel on silicon for high-performance vertical transistors," Nature **488**(7410), 189–192 (2012).
[8]M. Hocevar, G. Immink, M. Verheijen, N. Akopian, V. Zwiller, L. Kouwenhoven, and E. Bakkers, "Growth and optical properties of axial hybrid III-V/silicon nanowires," Nat. Commun. **3**, 1266 (2012).
[9]J. Justice, C. Bower, M. Meitl, M. B. Mooney, M. A. Gubbins, and B. Corbett, "Wafer-scale integration of group III-V lasers on silicon using transfer printing of epitaxial layers," Nat. Photonics **6**(9), 610–614 (2012).

[10]C. D. Bessire, M. T. Björk, H. Schmid, A. Schenk, K. B. Reuter, and H. Riel, "Trap-assisted tunneling in Si-InAs nanowire heterojunction tunnel diodes," Nano Lett. **11**(10), 4195–4199 (2011).
[11]W. S. Ko, I. Bhattacharya, T. T. D. Tran, K. W. Ng, S. Adair Gerke, and C. Chang-Hasnain, "Ultrahigh responsivity-bandwidth product in a compact InP nanopillar phototransistor directly grown on silicon," Sci. Rep. **6**, 33368 (2016).
[12]G. Otnes and M. T. Borgström, "Towards high efficiency nanowire solar cells," Nano Today **12**, 31–45 (2017).
[13]G. Mariani, A. C. Scofield, C. H. Hung, and D. L. Huffaker, "GaAs nanopillar-array solar cells employing in situ surface passivation," Nat. Commun. **4**, 1497 (2013).
[14]F. Qian, Y. Li, S. Gradečak, H. G. Park, Y. Dong, Y. Ding, Z. L. Wang, and C. M. Lieber, "Multi-quantum-well nanowire heterostructures for wavelength-controlled lasers," Nat. Mater. **7**(9), 701–706 (2008).
[15]Y. J. Lu, C. Y. Wang, J. Kim, H. Y. Chen, M. Y. Lu, Y. C. Chen, W. H. Chang, L. J. Chen, M. I. Stockman, C. K. Shih *et al.*, "All-color plasmonic nanolasers with ultralow thresholds: Autotuning mechanism for single-mode lasing," Nano Lett. **14**(8), 4381–4388 (2014).
[16]Y. Zhang, J. Wu, M. Aagesen, and H. Liu, "III-V Nanowires and nanowire optoelectronic devices," J. Phys. D. Appl. Phys. **48**(46), 463001 (2015).
[17]H. Kim, W. J. Lee, A. C. Farrell, J. S. D. Morales, P. Senanayake, S. V. Prikhodko, T. J. Ochalski, and D. L. Huffaker, "Monolithic InGaAs nanowire array lasers on silicon-on-insulator operating at room temperature," Nano Lett. **17**(6), 3465–3470 (2017).
[18]F. Lu, I. Bhattacharya, H. Sun, T.-T. D. Tran, K. W. Ng, G. N. Malheiros-Silveira, and C. Chang-Hasnain, "Nanopillar quantum well lasers directly grown on silicon and emitting at silicon-transparent wavelengths," Optica **4**(7), 717 (2017).
[19]N. Anttu and H. Q. Xu, "Efficient light management in vertical nanowire arrays for photovoltaics," Opt. Express **21**(S3), A558 (2013).
[20]J. Wallentin, N. Anttu, D. Asoli, M. Huffman, I. Åberg, M. H. Magnusson, G. Siefer, P. Fuss-Kailuweit, F. Dimroth, B. Witzigmann *et al.*, "InP nanowire array solar cells achieving 13.8% efficiency by exceeding the ray optics limit," Science **339**(6123), 1057–1060 (2013).
[21]W. Wei, X. Bao, C. Soci, Y. Ding, Z. Wang, and D. Wang, "Direct heteroepitaxy of vertical InAs nanowire array on Si (111) substrates for broadband photovoltaics and photodetection," Nano Lett. **9**(8), 2926–2934 (2009).
[22]J. L. Pura, J. Anaya, J. Souto, Á. C. Prieto, A. Rodríguez, T. Rodríguez, and J. Jiménez, "Local electric field enhancement at the heterojunction of Si/SiGe axially heterostructured nanowires under laser illumination," Nanotechnology **27**(45), 455709 (2016).
[23]J. L. Pura, J. Anaya, J. Souto, A. C. Prieto, A. Rodríguez, T. Rodríguez, P. Periwal, T. Baron, and J. Jiménez, "Electromagnetic field enhancement effects in group IV semiconductor nanowires. A Raman spectroscopy approach," J. Appl. Phys. **123**(11), 114302 (2018).
[24]J. L. Pura, J. Souto, P. Periwal, T. Baron, and J. Jiménez, "Electromagnetic field enhancement on axially heterostructured NWs: The role of the heterojunctions," J. Electron. Mater. **47**, 5072–5076 (2018).
[25]K. Aoki, E. Anastassakis, and M. Cardona, "Dependence of Raman frequencies and scattering intensities on pressure in Gasb, InAs, and Insb semiconductors," Phys. Rev. B **30**(2), 681–687 (1984).
[26]J. L. Pura, P. Periwal, T. Baron, and J. Jiménez, "Growth dynamics of SiGe nanowires by the vapour-liquid-solid method and its impact on SiGe/Si axial heterojunction abruptness," Nanotechnology **29**(35), 355602 (2018).
[27]S. Prucnal, M. Glaser, A. Lugstein, E. Bertagnolli, M. Stöger-Pollach, S. Zhou, M. Helm, D. Reichel, L. Rebohle, M. Turek *et al.*, "III-V semiconductor nanocrystal formation in silicon nanowires via liquid-phase epitaxy," Nano Res. **7**(12), 1769–1776 (2014).
[28]C. Bru-Chevallier, A. El Akra, D. Pelloux-Gervais, H. Dumont, B. Canut, N. Chauvin, P. Regreny, M. Gendry, G. Patriarche, J. M. Jancu *et al.*, "InGaAs quantum dots grown by molecular beam epitaxy for light emission on Si substrates," J. Nanosci. Nanotechnol. **11**(10), 9153–9159 (2011).
[29]S. Adachi, "Optical dispersion relations for GaP, GaAs, GaSb, InP, InAs, InSb, Al x Ga 1–x As, and In 1–x Ga x As y P 1–Y," J. Appl. Phys. **66**(12), 6030–6040 (1989).